Influence of Nickel-Iron Electrode Properties and Joint Shapes on Welded Joint Strength of Pearlitic Nodular Iron

The new nickel-iron electrode improved the joint strength of pearlitic nodular iron, and the single-U joint was found to have the lowest tensile strength

BY X. Y. ZHANG, Z. F. ZHOU, Y. M. ZHANG, S. L. WU and L. Y. GUAN

ABSTRACT. The influence of nickel-iron electrode properties and joint shapes on QT600-3 nodular iron joint strength and cracking was investigated using the Moiré fringe method. The total displacement of these welded joints under uniaxial tension was obtained. It was found that the newly developed nickel-iron electrode improved the welded joint strength. The experimental results also showed that double-V joint strength was higher than single-V joint strength, whereas single-U joint strength was lower than single-V joint strength. Single-U joint fracture was in the partially mixed zone of the weld root and parallel to the fusion line. This could be attributed to the complex compositions and structures at the weld root.

Introduction

The tensile strength values of QT600-3 nodular iron joints welded with the ENiFe-Cl electrodes are low in comparison with those of the base metal, which has attracted much attention from researchers (Refs. 1–9). The early work was concerned with the postweld heat treatment (annealing or normalizing) of these welded joints, but results were unsatisfactory (Refs. 7–9). And then the displacement and strain of these welded joints under uniaxial tension were studied using the Moiré fringe method (Ref. 10). The lower yield strength of the weld metal was found to be one of the reasons causing the low strength of these welded joints. In order to improve the weld metal properties, a new nickel-iron electrode, whose yield and tensile strength reached those of high-strength nodular iron QT600-3, was developed (Ref. 11). Therefore, it is of great significance to continue research on the influence of the electrode yield strength and different joint shapes on improving welded joint strength.

X. Y. ZHANG, Z. F. ZHOU, Y. M. ZHANG, S. L. WU and L. Y. GUAN are with the Welding Division, Jilin University of Technology, Changchun, China.

Experimental Materials and Method

The test plates chosen were pearlitic nodular iron QT600-3, which had dimensions of 120 x 70 X 20 mm (4.8 x 2.8 x 0.8 in.). The experimental electrode was a newly developed nickel-iron electrode (Ref. 11) with a core diameter of 3.2 mm (1/8 in.). The chemical composition and mechanical properties of the nodular iron and deposited metal are listed in Tables 1 and 2, respectively. For the convenience of comparison, these two tables also include the composition and mechanical properties of the ENiFe-Cl electrode.

Single-V, double-V and single-U grooves were machined separately in the nodular iron plates, as shown in Fig. 1. Two plates were placed 2 mm (0.08 in.) apart and two tack welds were made at the ends to fix the plates. The butt joints were then continuously welded with a shielded metal arc multipass welding process. The experimental welding machine was operated on AC at 120 A. The welding speed was 2.5 mm/s (0.1 in./s). No preheating was used and the interpass temperature was about 600°C (1112°F).

The specimen was cut along the transverse direction of the welded plate and machined into lath form with dimensions of 130 x 14.5 x 1.38 mm (5.2 x 0.58 x 0.055 in.). Moiré fringe grids with the density of 100 lines/mm and 80 X 15 mm (3.2 x 0.6 in.) in size were placed on each side of the specimen joint, so the transverse and longitudinal deformation fringes of the welded joint under uniaxial tension could be obtained.

The photographs of the Moiré fringe patterns were taken of the welded joint area using a Moiré fringe experimental machine. The displacement of the welded joint was measured using a JTT-50 projective device. According to the Prandtl-Reuss increment theory, which states the total strain increment during the plastic deformation period is equal to the elastic strain increment plus the plastic strain increment (Ref. 12), the total field strain and stress distribution of these joints was acquired.

KEY WORDS

QT600-3 Nodular Iron
Nickel-Iron Electrode
Welded Joint Strength
Moiré Fringe Method
Single-V Joint
Double-V Joint
Single-U Joint

Experimental Results and Discussion

Influence of Nickel-Iron Electrode Properties on Nodular Iron Joint Strength

The displacement, strain and stress of QT600-3 nodular iron joints welded using the ENiFe-Cl electrodes with a yield strength of 340 MPa were discussed in Ref. 10. In the current work, the single-V joint (Fig. 1A), the same joint type as that in Ref. 10, was selected to study the displacement and strain of QT600-3 nodular iron joints welded with the

newly developed nickel-iron electrodes. This can then be used to compare the effect of the different electrodes on the welded joint strength.

Displacement Analysis

Figure 2 shows the Moiré fringe patterns of a single-V joint under uniaxial tension. When the tensile stress was lower, the fringes in the weld and base metal were relatively even, but the shape was like "\ /" — Fig. 2A. Even when the tensile stress reached 342.80 MPa, the uneven distribution of the fringes was only caused by the different elastic modulus of the weld and base metal, so there was no obvious increase of the fringes in the weld, as shown in Fig. 2B. When the tensile stress reached 428.55 MPa, both the weld and base metal yielded. No obvious increase of the fringes in the weld was observed — Fig. 2C. However, with the further increase of the tensile stress, the fringes in the weld increased faster than those in the base metal because the weld had better plasticity (7.35%) than the base metal (2.5%). In critical tension stress, the fringes in the weld are more dense than those in the base metal, as shown in Fig. 2D.

Compared with Fig. 7 in Ref. 10, it is apparent that the Moiré fringe change of the joint welded with the new nickel-iron electrodes was much different from that with ENiFe-Cl electrodes. Firstly, under the lower tensile stress, the weld fringes of the joint welded with the ENiFe-Cl electrodes increased faster. When the tensile stress reached 340 MPa the weld yielded, but the base metal did not yield, so the deformation of the joint mainly focused on the weld, where the fringes increased significantly more, resulting in an extremely uneven fringe distribution. As the tensile stress reached 439.0 MPa, the joint failed due to the stress concentration at the weld root. Secondly, with the ENiFe-Cl electrodes, the uneven distribution of the joint fringes was more serious and the weld fringes were more dense in critical fracture stress, which were caused by the differences in elastic modulus, yield strength and elongation between the weld and the base metal. Finally, the average tensile strength of the joint welded with the ENiFe-Cl electrodes was 417.2 MPa (Ref. 13), while that using the new electrodes was much higher.

Strain Analysis

Figure 3 shows the transverse strain (ε_x) distribution on several sections under 465.27 and 477.55 MPa tensile stress. The deformation of the welded specimens under uniaxial tension was symmetrical along the centerline of the weld transverse section so half of a specimen was taken for analysis. X shows the distance from the weld centerline, and Y is the centerline of the weld transverse section. It is interesting to note that, under the same tensile stress, the weld strain of the joint welded with the new electrode was much smaller than that of the ENiFe-Cl electrode and the peak value of the strain at the weld root was lower. For example, on the section Y = 0, the maximum strain of the joint welded with the new electrodes under 465.27 MPa tensile stress was 22.2 x 10^{-3}, while that of the ENiFe-Cl electrodes under 401.04 MPa tensile stress had reached 27.6 x 10^{-3} (Ref. 10). The reasons were that the ENiFe-Cl electrodes had lower yield strength and better plasticity than the new electrodes. Therefore, the weld of the ENiFe-Cl electrodes was easy to deform and the strain concentration was more obviously at the weld root, which also resulted in the welding joint cracking under the lower tensile stress (439.0 MPa). With the new electrodes, the joint cracked vertically along the section in which X = 4.14 mm under 484.86 MPa tensile stress, as shown in Fig. 4. It is obvious that the welding joint strength increased by at least 10%.

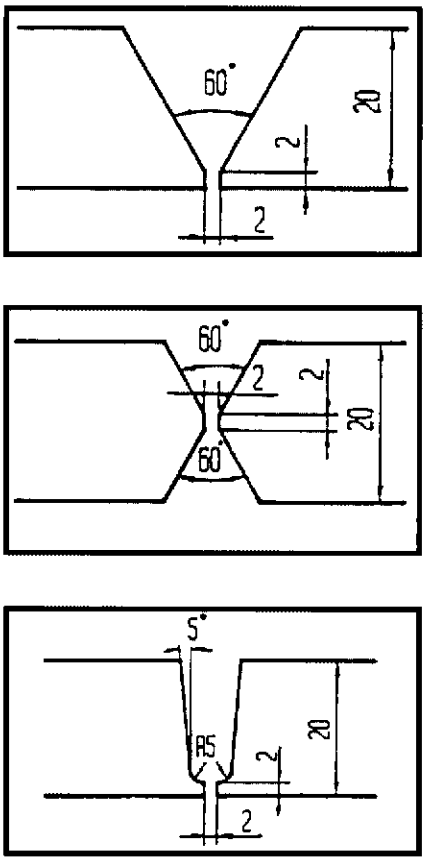

Fig. 1 — Joint shape and dimensions.

Influence of Joint Shapes on Nodular Iron Joint Strength

The Moiré fringe patterns of a double-V joint welded with the new electrodes under different tensile stresses are shown in Fig. 5. Because the two groove faces of a double-V joint are symmetrical, the deformation is relatively even compared with that of a single-V joint, as shown in Fig. 5A. The joint fringes distributed evenly and parallel to each other and the displacement at any point was basically the same. But with the increase of the

Table 1 — Chemical Composition of the Deposited Metal (wt-%)

Materials	C	Si	Al	Ti	Nb	Co	Mo	W	V	Y	ΣRe	Ni	Fe
New nickel-iron electrode	2.27	1.18	0.24	0.40	0.18	0.29	—	—	—	0.0021	—	46.8	surplus
ENiFe-Cl electrode	2.21	1.10	0.24	0.52	0.25	0.42	0.13	0.09	0.62	—	0.017	46.2	surplus

Table 2 — Mechanical Properties of the Nodular Iron and the Deposited Metal

Materials	Yield Strength σ_s MPa	Tensile Strength σ_s MPa	Elastic Modulus E MPa	Poisson's Ratio υ	Elongation δ %
QT600-3 nodular iron	420	640	180000	0.28	2.5–3.5
New nickel-iron electrode	414.93	632.1	165000	0.29	7.35
ENiFe-Cl electrode	340	600	160000	0.32	8–9

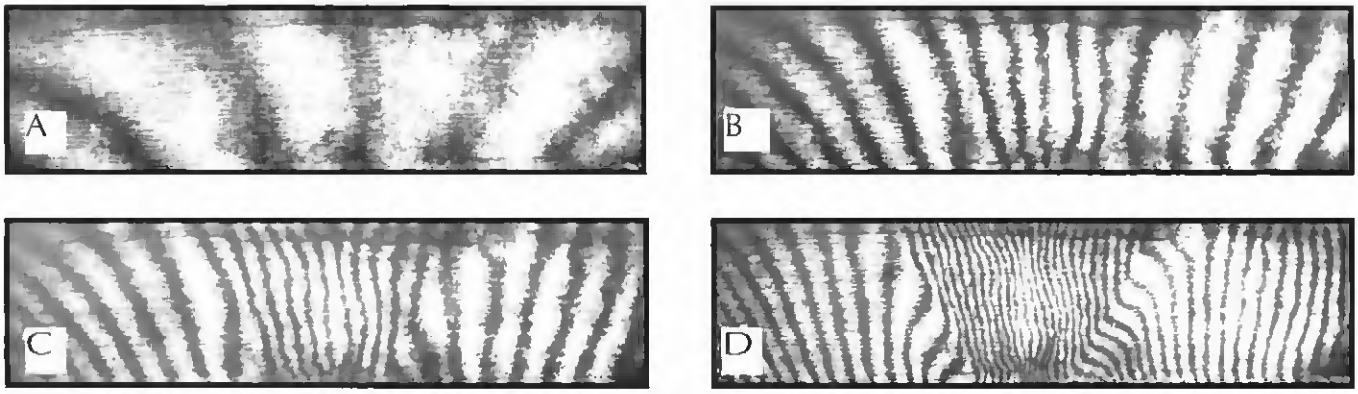

Fig. 2 — Moiré fringe patterns of a single-V joint under different tensile stresses. A — 146.90 MPa; B — 342.80 MPa; C — 428.55 MPa; and D — 477.55 MPa.

tensile stress, the fringes in the weld increased faster and became denser than those in the base metal (Fig. 5B–D) as the weld had a lower elastic modulus and better plasticity than the base metal. When the tensile stress reached 490.26 MPa, the tensile specimen was broken. The crack initiated immediately at the root in the middle of the weld and propagated along the direction that was vertical to the maximum tensile stress direction, as shown in Fig. 6. It is possible that the local environment became more aggressive because of the reduced deposited metal content in the middle of the joint. If the total deformation was constant, the strain in the middle of the joint should be larger than that in the other zone.

Figure 7 shows the Moiré fringe-patterns of a single-U joint welded with the new electrodes under different tensile stresses. No difference was discernible between single-U and single-V joints under the lower tensile stress (Fig. 7A). As the tensile stress increased, the fringe distribution in the single-U joint was more even than that in the single-V joint due to the smaller angle of the single-U groove. But it is noted that the deformation in the zone between the weld and the base metal was very small and the Moiré fringes were very sparse. The Moiré fringes in the weld were more dense so the stress concentrated at the weld root. When the tensile stress reached 388.89 MPa, the tensile specimen failed without a large amount of deformation as shown in Fig. 8. The crack was in the partially mixed zone and was basically parallel to the fusion line. In general, the stress concentration at the weld root of the single-U joint is smaller than that of the single-V joint and the tensile strength of the single-U joint should be higher. However, the experimental results showed that the single-U joint cracked in the partially mixed zone under the lower tensile stress.

With regard to the cracking of the single-U joint under uniaxial tension, it is likely that the partially mixed zone played an important role in the tensile strength of the welded joint. This verifies the earlier work of Zhang, *et al.* (Ref. 10), who concluded that complex chemical compositions and microstructure in the partially mixed zone could be a factor leading to the welded joint cracking. When the groove angle is small, the partially mixed zone is almost vertical to the tensile stress direction. As soon as the crack initiates, the crack propagates along this zone consuming the minimum energy. Therefore, improvements to the chemical compositions and microstructure in the partially mixed zone will assist to increase the welding joint strength.

Experiments on a series of tensile specimens of QT600-3 nodular iron joints welded with the new nickel-iron electrodes were carried out using the Moiré fringe method. The tensile strength values of these tensile specimens are listed in Table 3. With the new electrodes, the average tensile strength of the single-V joint was 483.17 MPa, and the strength coefficient of the joint (welded joint/base metal tensile strength) was 0.78. While the average tensile strength of a single-V joint welded with the ENiFe-CI electrodes was only 417.2 MPa, the strength coefficient of the joint was 0.67.

When examining the tensile strength of the other joints welded with the new electrodes, it was found that the average tensile strength of a double-V joint was 487.27 MPa and the joint strength coefficient was 0.79, and that of the single-U joint was 397.47 MPa and the joint strength coefficient was 0.64. So the double-V joint had the highest tensile strength and the single-U joint had the lowest one.

Table 3 — Tensile Strength of Welded Joint Specimens

Electrode	Joint Shape	Specimen No.	Tensile Strength Unit (MPa)	Tensile Strength Average (MPa)
New nickel-iron electrode	Single-V	1	484.86	
		2	481.24	483.17
		3	483.40	
	Double-V	1	490.26	
		2	482.36	487.27
		3	489.20	
	Single-U	1	394.06	
		2	405.03	
		3	401.90	397.47
		4	388.89	

Conclusions

1) The influence of the nickel-iron electrode properties and the joint shapes on the welded joint strength of QT600-3 nodular iron under uniaxial tension was studied using the Moiré fringe method.

2) When the yield strength of the nickel-iron electrode changed from 340 to 414.93 MPa, the tensile strength of the welded joint increased from 417.2 to 487.27 MPa, and the strength coefficient of the joint increased from 0.67 to 0.79.

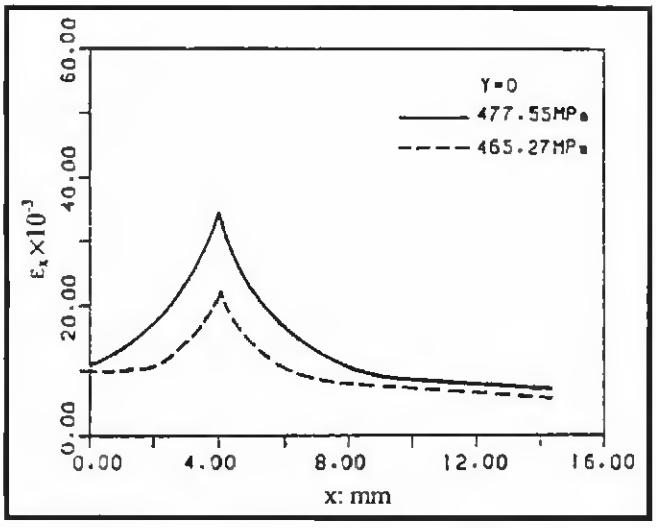

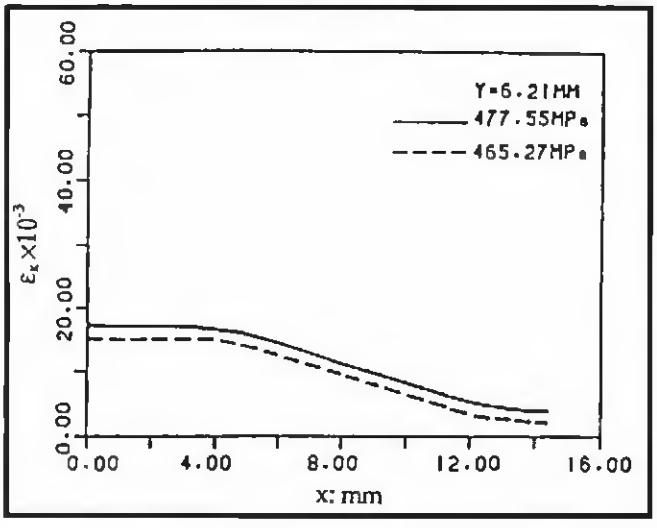

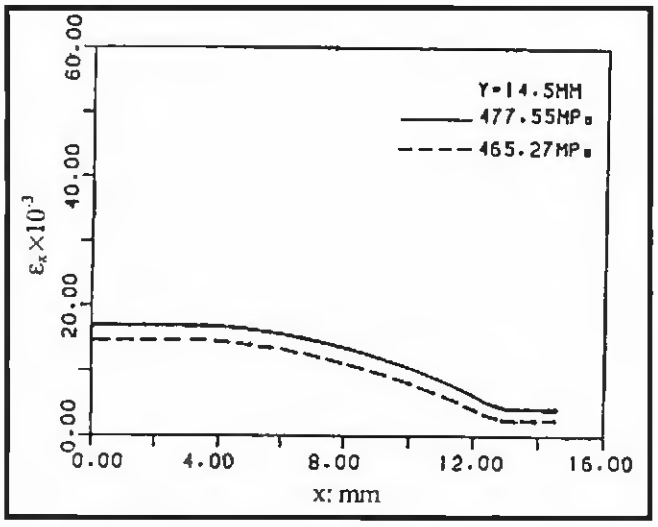

Fig. 3 — The change of transverse strain on several sections under 465.27 and 477.55 MPa tensile stress.

Fig. 4 — Side view of single-V joint fracture.

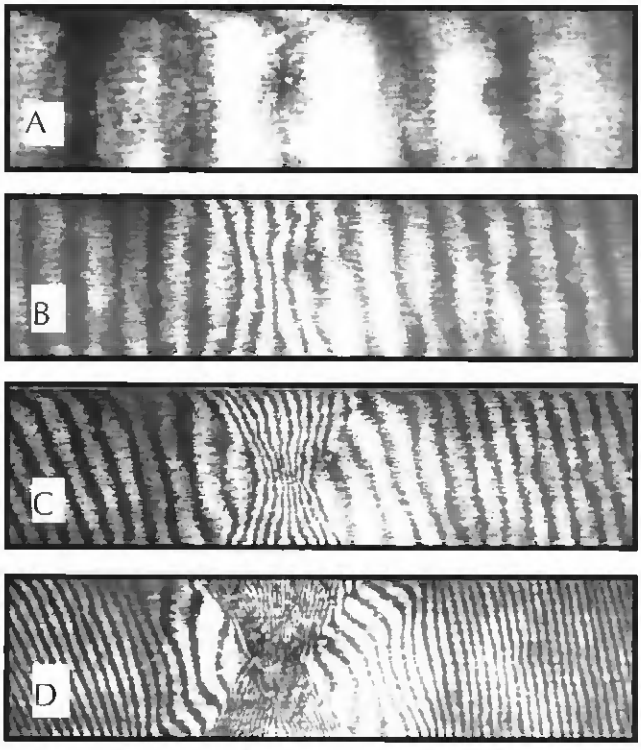

Fig. 5 — Moiré fringe patterns of double-V joint under different tensile stresses. A — 158.17 MPa; B — 368.97 MPa; C — 421.96 MPa; and D — 482.36 MPa.

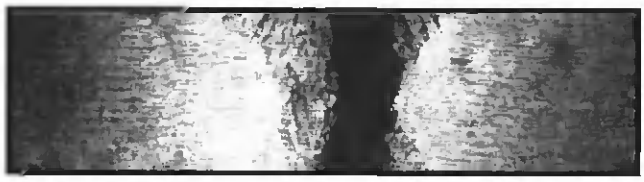

Fig. 6 — Side view of double-V joint fracture.

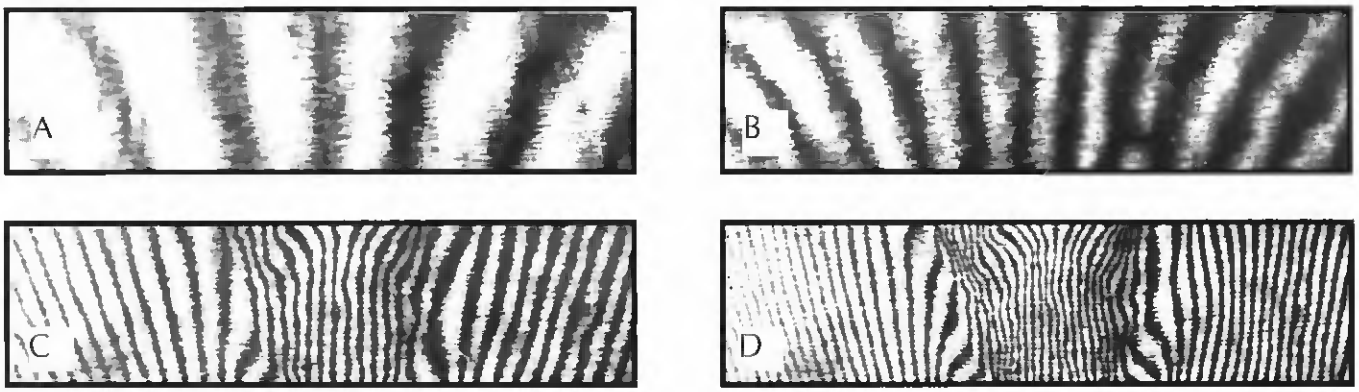

Fig. 7 — Moiré fringe patterns of single-U joint under different tensile stresses. A — 155.56 MPa; B — 259.26 MPa; C — 362.96 MPa; and D — 383.70 MPa.

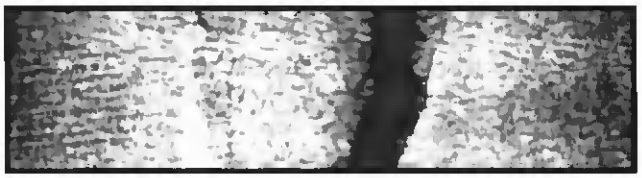

Fig. 8 — Side view of single-U joint fracture.

It is obvious that the electrode properties brought closer to the base metal improved the welded joint strength.

3) The double-V joint welded with the new nickel-iron electrodes had the highest tensile strength, followed by the single-V and the single-U joint. Single-U joint fracture was in the partially mixed zone of the weld root and parallel to the fusion line, which further revealed the effect of the partially mixed zone on joint cracking.

References

1. Osborn, A. J. 1977. The repair welding of ductile cast irons. *Casting Engineering,* (3).

2. Anant Narayan, S. N., *et al.* 1979. Weldability of spheroidal-graphite type Ni-resist cast irons. *Foundry Trade J.* July 5, pp. 17–45.

3. Griffing, L. 1972. *Welding Handbook.* Sixth Edition. The American Welding Society, Miami, Fla.

4. Bishel, R. A., and Conaway, H. R. 1976. Flux cored arc welding for high-quality joints in ductile iron. *AFS Transactions,* (4).

5. Forrest, R. D. 1983. Welding ductile iron castings. *Casting Engineering & Foundry World,* (4).

6. Thornaycroft, D. R. 1963. Welding of spheroidal-graphite iron. *Foundry Trade Journal,* 25 (4).

7. Flannery, J. W. 1968. Welding ductile iron-part one. *Welding Engineer,* (11).

8. Ball, F. A., *et al.* 1954. Metallic arc welding of spheroidal graphite cast iron. *Foundry Trade Journal,* (10).

9. Voigt, R. C., and Loper, C. R. 1986. Welding metallurgy of grey and ductile cast irons. *AFS Transactions.*

10. Zhang, X. Y., Zhou, Z. F., *et al.* 1992. Crack initiation and propagation in a pearlitic nodular iron joint welded with a nickel-iron electrode. *Welding Journal,* (8).

11. Zhang, X. Y., and Zhou, Z. F., *et al.* 1995. A newly developed nickel-iron electrode with superior hot cracking resistance and high-strength properties for welding pearlitic nodular iron. *Welding Journal,* 74 (1): 16-s to 20-s.

12. Bing, S., *et al.* 1986. Measuring and calculating the plastic stress deformation by the Moiré fringe method. *Proceeding of the Third Annual Meeting of Forging Institute of Chinese Mechanical Engineering Society.*

13. Zhang, X. Y. 1991. A study of the joint strength of QT600-3 nodular iron welded with nickel-iron electrodes. Ph. D. Dissertation (in Chinese).